nature neuroscience

Intention and attention: different functional roles for LIPd and LIPv

Yuqing Liu, Eric A Yttri & Lawrence H Snyder

Establishing the circuitry underlying attentional and oculomotor control is a long-standing goal of systems neuroscience. The macaque lateral intraparietal area (LIP) has been implicated in both processes, but numerous studies have produced contradictory findings. Anatomically, LIP consists of a dorsal and ventral subdivision, but the functional importance of this division remains unclear. We injected muscimol, a $GABA_A$ agonist, and manganese, a magnetic resonance imaging lucent paramagnetic ion, into different portions of LIP, examined the effects of the resulting reversible inactivation on saccade planning and attention, and visualized each injection using anatomical magnetic resonance imaging. We found that dorsal LIP (LIPd) is primarily involved in oculomotor planning, whereas ventral LIP (LIPv) contributes to both attentional and oculomotor processes. Additional testing revealed that the two functions were dissociable, even in LIPv. Using our technique, we found a clear structure-function relationship that distinguishes LIPv from LIPd and found dissociable circuits for attention and eye movements in the posterior parietal cortex.

We sought to distinguish between circuits dedicated to general perception and circuits specialized for directing particular movements. LIP has been implicated in both saccade planning and attentional processing, with conflicting evidence from single-unit recording[1–4], intracortical microstimulation[5,6], anatomical studies[7–10], surgical lesions[11] and reversible inactivation[12–15]. Ambiguities arise because attention and eye movements are tightly coupled. Although attention can be disengaged from the point of fixation[16], primates usually look at objects of interest[17]. However, even when subjects attend to a peripheral target without looking directly at it, oculomotor planning activity probably occurs nonetheless[18–20]. We examined the role of LIP in these processes and asked whether attention and oculomotor planning rely on shared or distinct neuronal substrates.

Although LIP is often treated as a whole, it is actually composed of two separate areas, LIPd and LIPv. The distinction is based on patterns of myelination, connectivity and immunohistochemistry[21–23]. LIPv, deep in the lateral bank of the intraparietal sulcus (IPS), is characterized by dense myelination, whereas LIPd, which is superficial to LIPv, is lightly myelinated[22,23]. LIPv is more strongly connected with visual area V3, posterior intraparietal area (PIP) and parietal-occipital area (PO), whereas LIPd is more strongly connected with visual area V4, V4 transitional area (V4t), area TEa plus TEm (TEa/m), temporal parietal occipital area (rostral,TPOr), and Walker area 45 (ref. 21). Both are reciprocally connected to frontal eye fields (FEF)[21,23]. Conflicting results regarding the role of LIP could occur if LIPd and LIPv serve different functions and previous studies sampled them differently. To address this possibility, we tested whether LIPd and LIPv have different roles in oculomotor and attentional processing.

Single-unit recording is frequently used to explore structure-function relationships. However, the determination of what structure one is recording from is often partially based on the functional properties being recorded, and this circularity can lead to uncertainty. This can be ameliorated by reconstructing the recording sites on the basis of post-mortem landmarks, reconstructing the electrode trajectories from stereotaxic data or directly imaging the electrode *in vivo*[24].

Recording techniques coupled with recording site reconstruction can find correlations between neural activity and particular task conditions but do not directly address the causal role neurons may have in behavior. More information can be obtained by lesioning the area and observing any deficiencies that arise. As with unit recording, proper interpretation requires accurate localization of the lesion. We achieved this by injecting both muscimol and manganese. Muscimol, a $GABA_A$ agonist, increases local inhibition and thereby attenuates local activity. The manganese can be imaged using magnetic resonance imaging (MRI)[25], providing direct *in vivo* visualization of the injection site.

We found that LIPd and LIPv have different roles in saccade planning and covert attention. Lesions of LIPd affected saccades, but not search, whereas lesions of LIPv affected both saccades and search. Our findings suggest that oculomotor and attentional processes in LIPv can be dissociated at the neural circuit level.

RESULTS

LIP lesions impair both saccades and search

After mapping out LIP on the basis of standard functional criteria (see Online Methods), we performed 35 reversible inactivations in three monkeys using 1–4 µl of 8.0 mg ml^{-1} muscimol mixed with 19.8 mg ml^{-1} $MnCl_2(H_2O)_4$. We tested the effects of each lesion on

Department of Anatomy and Neurobiology, Washington University School of Medicine, St. Louis, Missouri, USA. Correspondence should be addressed to Y.L. (yuqing@eye-hand.wustl.edu).

Received 17 December 2009; accepted 5 January 2010; published online 28 February 2010; corrected online 7 March 2010 (details online); doi:10.1038/nn.2496

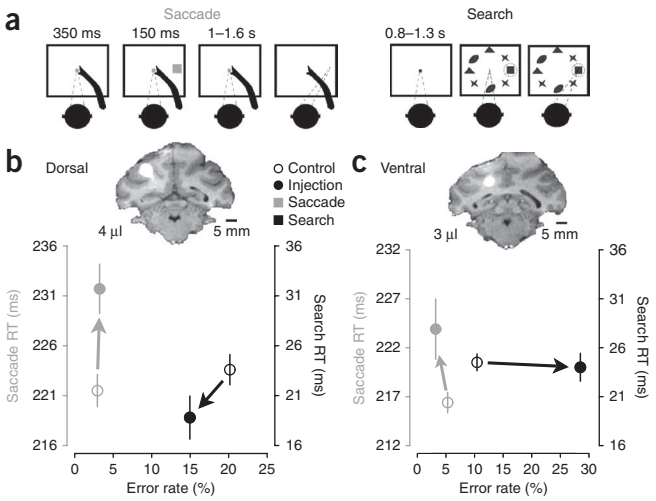

Figure 1 Behavioral tasks and example injections. (**a**) Schematic of the memory-guided saccade and the visual search task. Saccades were directed to remembered target locations after a 1–1.6-s memory period. The visual search task was based on a previously described task[13,15]. On two-thirds of trials, monkeys performed a single saccade directly to a purple target (a square) lying in a radial array of seven purple distractors (ellipses, crosses and triangles). For the remaining trials, the target appeared alone, without distractors (data not shown), as a control for the oculomotor effect. (**b**,**c**) MRIs, reaction times (RT) and error rates from two example injections placed at different depths in the lateral bank of the IPS. Manganese mixed with muscimol resulted in a bright halo, seen here in coronal slices. Scale bars represent 5 mm. The mean of saccade (gray) and search (black) reaction times from each injection (solid circles) and their matched controls (hollow circles) are plotted against their corresponding error rates. Arrows indicate the effects of each inactivation in the reaction time and error rate domains. Upward and rightward directions indicate impaired behavior.

a standard memory-guided saccade task and a visual-search task (**Fig. 1a**). A visual search protocol is useful for measuring attentional effects, as visual search generally requires the use of limited resources for information processing[26] and attention is thought to operate most strongly when distinguishing a target from distractors[27].

The muscimol lesions affected both saccadic and search performance (**Fig. 1**), with the former occurring about twice as frequently as the latter. A 4-µl injection close to the gyral surface (**Fig. 1b**) increased saccade reaction time by 10.2 ms compared with control sessions ($P = 7.6 \times 10^{-4}$, two-sided Welch's t test). This injection did not significantly affect saccade error rate (experimental – control rates = 0.3%, $P = 1.0$, two-sided Fisher test; **Fig. 1b**). There were small improvements in search error rate (−5.2%, $P = 0.28$, two-sided χ^2 test) and search reaction time (−4.8 ms, $P = 0.06$) (**Fig. 1b**). In contrast, a second, 3-µl injection, deeper in the sulcus (**Fig. 1c**) not only significantly impaired saccades (7.5 ms slowing, $P = 0.024$; change in error rate was not significant, $P = 0.28$) but also impaired search (+18.1% error rate, $P < 2 \times 10^{-8}$; change in reaction time was not significant, $P = 0.78$). Unless otherwise noted, we report lesion effects on saccades and search only to contralateral targets.

Search is impaired by LIPv, but not LIPd lesions

The two example injections, one shallow and one deep into the IPS sulcus (**Fig. 1b**,**c**), had different effects on visual search. To test for a systematic effect of lesion depth on search, we plotted error rate against normalized depth for each injection (see Online Methods and **Fig. 2a**). Anatomical data suggest that the LIPd/v boundary lies at 53% of full sulcal depth[22] (6.8 mm for our monkeys; see Online Methods). No injections above this border (**Fig. 2b**) produced significant search effects (all $P > 0.1$ for error increase cases), whereas 72% (13 of 18) of deeper injections significantly increased search errors ($P < 0.05$). This was also true for the data from each of the three monkeys considered individually (**Table 1**); no shallow injections affected search, whereas five out of seven, six out of eight and two out of three of the deep injections impaired search. The difference in errors between shallow (LIPd, −0.2 ± 1.4%, $P = 0.86$) and deep (LIPv, 15.7 ± 3.4%, $P = 6.1 \times 10^{-5}$) injections was highly significant ($P = 5.3 \times 10^{-5}$, two-sided permutation test). There was a similar, although nonsignificant, trend in search reaction time, with LIPd lesions having almost no effect (−0.65 ms, $P = 0.6$) and LIPv lesions slowing responses by 6.6 ms ($P = 0.35$). Thus, LIPv, but not LIPd, lesions impaired visual search.

In contrast with search effects, saccade effects occurred after both LIPd and LIPv lesions. Memory-guided saccades were impaired (either slowed reaction time or increased error rate, $P < 0.025$, two-sided Welch's t test and χ^2 test) in 12 of 17 (70.6%) LIPd injections and 13 of 18 (72.2%) LIPv injections (**Figs. 2c** and **3a**,**b**), and there was no linear trend in the effect size as a function of depth (Pearson correlation coefficient $r = -0.031$, $P = 0.86$; **Fig. 2c**). For comparison, the search data did have a linear trend ($r = 0.64$, $P = 0.0001$). At a population level, the effect on mean adjusted reaction time (a measure combining reaction time and error effects; see **Supplementary Text** and **Supplementary Fig. 1**) for saccades was similar for LIPd (11.1 ± 1.8 ms, $P = 9.2 \times 10^{-5}$) and LIPv (10.1 ± 2.0 ms, $P = 5.3 \times 10^{-5}$). Similar effects were found on visually guided saccades in both LIPd ($n = 2$, mean reaction time effect = 8.3 ms) and LIPv ($n = 6$, reaction time effect = 9.8 ± 4.9 ms, $P = 0.094$), demonstrating that the deficit was not specific to working memory. Effects on saccade accuracy, precision, duration and error rate were small or absent in both LIPd and LIPv (see **Supplementary Text**, **Supplementary Fig. 2** and **Supplementary Table 1**).

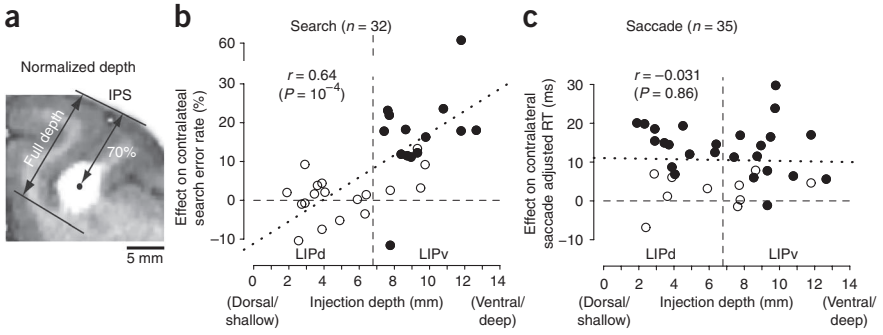

Figure 2 LIP lesion effects as a function of depth. (**a**) An illustration of how the full IPS depth and the lesion depth were measured for an LIPv injection from a coronal MRI slice. (**b**) Lesion-induced contralateral search error rate as a function of normalized injection depth. Filled circles represent injection sites with significant effects of either reaction time or errors ($P < 0.025$ before correction for the two independent comparisons). The vertical dashed line approximates the LIPd/v border. The mean LIPd effect was a change in error rate of –0.2 ± 1.4% and the mean LIPv effect was 15.7 ± 3.4%. (**c**) Contralateral adjusted saccade reaction time effect (see **Supplementary Text**) as a function of injection depth. Mean effects in LIPd and LIPv were 11.1 ± 1.8 ms and 10.1 ± 2.0 ms, respectively. Dotted lines are least-squares regression fits for the data, respectively. Four data points were shifted slightly to avoid overlap in **b**.

Table 1 Effect of reversible lesions on search performance

	Mean of G,Q and W		Monkey G		Monkey Q		Monkey W	
Effect on search	Significance	Mean	Significance	Mean	Significance	Mean	Significance	Mean
LIPd	0 of 14 (0%)	−0.2 ± 1.4	0 of 5 (0%)	−0.3 ± 3.2	0 of 7 (0%)	−1.6 ± 1.6	0 of 2 (0%)	3.0 ± 0.9
LIPv	13 of 18 (72.2%)	15.7 ± 3.4***	5 of 7 (71.4%)	13.9 ± 1.7*	6 of 8 (75%)	18.9 ± 7.4*	2 of 3 (66.7%)	11.1 ± 4.4

Entries show mean ± s.d. or percentage of sites that showed a significant increase in contralaterally directed search error rate ($P < 0.05$, two-sided χ^2 test).
***$P < 0.001$ and *$P < 0.05$.

Directional effects on saccades and search

The distinction between LIPd and LIPv was also apparent when individual target directions were considered. LIPd lesions did not affect search errors for targets in any single direction (mean = −2.3%, all $P > 0.4$ for increase of errors; **Fig. 3c**), whereas LIPv lesions significantly increased search errors for all three contralateral targets (12.3%, $P = 0.0004$; 13.8%, $P = 0.0009$; 12.6%, $P = 0.006$; **Fig. 3d**). Unlike search, saccades were impaired by lesions of either area, especially for contralateral directions (LIPd, 14.8, 8.5 and 13.0 ms, all $P < 0.03$; **Fig. 3e**; LIPv, 9.7, 11.9 and 7.6 ms, all $P < 0.004$; **Fig. 3f**). Lesions of LIPd and LIPv had similar effects on saccades in each individual direction (t tests, all $P \geq 0.2$) and on the pooled measure ($P = 0.72$).

The lesion effects were consistent across each of the three monkeys (**Tables 1** and **2**). All three monkeys showed markedly elevated contralateral saccade reaction time effects in both areas, which were significant in two monkeys ($P < 0.05$). In each of the three monkeys, the contralateral search effect was markedly elevated in LIPv (significant in two, $P < 0.05$) and nonsignificant (small or negative, $P > 0.18$) in LIPd. A two-way, direction × monkey ANOVA revealed no main effect of monkey on either the contralateral saccade reaction time effect (LIPd, $F_2 = 1.7$, $P = 0.2$; LIPv, $F_2 = 1.9$, $P = 0.16$) or the contralateral search error effect (LIPd, $F_2 = 0.52$, $P = 0.6$; LIPv, $F_2 = 0.23$, $P = 0.79$).

Saccade, but not search, effect depends on eye position

The retinotopic responses of LIP neurons are gain modulated by eye position[28]. To test whether eye position might modulate lesion effects, we had two monkeys perform the saccade and search tasks after a subset of injections with all visual stimuli, including the initial fixation target, displaced either 5° to the left or right of straight ahead (**Fig. 4a**). Saccade reaction times were slowed to a similar extent regardless of eye position in LIPd and LIPv (**Fig. 4b**,**c** and **Supplementary Table 2**). This was true for each individual injection, with significant effects of eye position on saccade reaction time occurring at only four of nine LIPd sites (two increased and two decreased reaction times with contralateral eye position) and one of nine LIPv sites (decreased reaction time with contralateral eye position), and was also true for the population (LIPd, 5.7 ± 3 ms versus 5.8 ± 1.6 ms, difference $P = 0.96$, paired t test; LIPv, 10 ± 2.5 ms versus 8.0 ± 2.9, difference $P = 0.24$).

There was no search effect in LIPd for either eye position (−2.1 ± 1.4%, $P = 0.18$; −0.55 ± 1.4%, $P = 0.7$; **Fig. 4b**). In LIPv, however, the error rate for search more than doubled for contralateral compared with ipsilateral eye position (11 sites tested, 16.8 ± 5.5% versus 5.4 ± 2.2%, difference $P = 0.034$, paired t test; **Fig. 4c**). At the individual injection level, 10 of 11 LIPv injections resulted in more search errors with contralateral compared with ipsilateral eye positions, and 6 of the 11 were significantly greater ($P < 0.02$, two-sided χ^2 test or Fisher exact test). Thus, the search effect depended on initial eye position in LIPv, whereas the saccade effect was independent of eye position in both areas.

Lesion overlap map and control experiments

To further characterize the anatomical locus of the search effect, we constructed three-dimensional (**Fig. 5a**,**b**) and two-dimensional (**Fig. 5c**) lesion overlap maps (see **Supplementary Text**) showing the 8 search-positive and 12 search-negative lesions from the two fascicularis monkeys. Search-positive effects (**Fig. 5b**,**c**) resulted from injections in the ventral (deep) portion of the intraparietal sulcus (IPS), whereas search-negative effects (**Fig. 5a**,**c**) resulted from dorsal (superficial) injections in the lateral bank, directly above the search-positive area. The voxels that are most frequently involved in search-positive or search-negative effects were separated by 3.0 mm. These results support the conclusion that search is impaired by LIPv, but not LIPd, injections.

To rule out alternative explanations for the origin of search effects, we performed nine control injections into the medial bank of the IPS (**Fig. 6a**,**b**). Neither large ($n = 4$; **Fig. 6a**) nor focal ($n = 5$; **Fig. 6b**) medial bank injections impaired search (mean effect = −0.36% and 1.2%, $P = 0.75$ and $P = 0.56$, respectively). To test whether search effects are produced by large inactivations independent of their locations, we picked five large LIPd injections with additional involvement of visual area 7a (**Fig. 6c**) out of 14 LIPd injections (**Fig. 6d**) and inspected their effects on search and

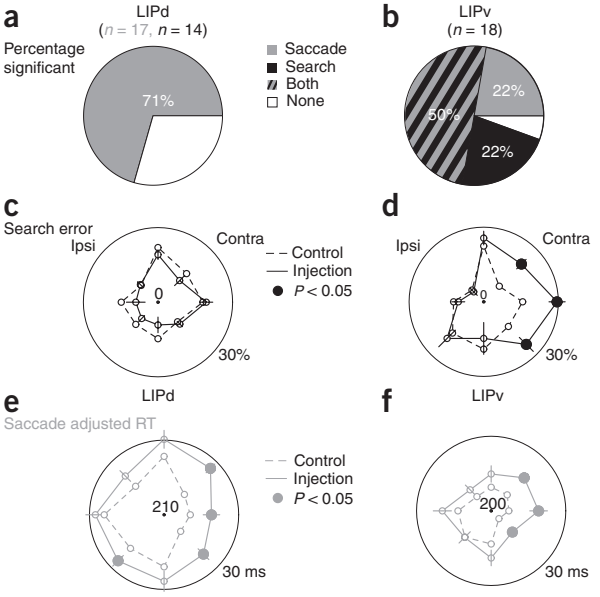

Figure 3 Performance of memory-guided saccades and visual search before and after LIPd and LIPv inactivations. (**a**,**b**) Prevalence of significant saccadic (gray) and/or search (black) effects following LIPd and LIPv lesions. (**c**–**f**) Mean search error rate (black) and adjusted saccade reaction time (gray) by target direction for LIPd and LIPv controls (dashed line) and injections (solid line). Large outer circles indicate 30% (search error rate) or 30 ms (saccade reaction time) beyond the center value. Error bars are ± s.e. of the difference between the control and injection values. Solid data points indicate significant effects ($P < 0.05$).

Table 2 Effect of reversible lesions on saccade performance

	Mean of G,Q and W		Monkey G		Monkey Q		Monkey W	
Effect on saccade	Reaction time	Error	Reaction time	Error	Reaction time	Error	Reaction time	Error
LIPd: effect	7.1 ± 1.6***	4.2 ± 1.6*	9.1 ± 2.9*	5.7 ± 3.1	5.0 ± 2.1+	4.5 ± 1.3*	6.7 ± 1.9	–2.9 ± 1.0
Significant sites (%)	12 of 17 (70.6%)		7 of 8 (87.5%)		4 of 7 (57.1%)		1 of 2 (50%)	
LIPv: effect	7.3 ± 1.9***	2.9 ± 1.6+	5.4 ± 2.6+	5.2 ± 3.1	6.9 ± 3.4*	3.2 ± 2.0	12.9 ± 4.1	–3.0 ± 2.3
Significant sites (%)	13 of 18 (72.2%)		6 of 7 (85.7%)		5 of 8 (62.5%)		2 of 3 (66.7%)	

Entries show mean ± s.d. or percentage of sites that showed a significant increase in either contralaterally directed saccade reaction time or error rate ($P < 0.05$, two-sided Welch's t test for reaction time comparison and χ^2 test for error comparison, corrected for multiple comparison of two).
***$P < 0.001$, *$P < 0.05$ and +$P < 0.1$.

saccades. These injections all significantly impaired saccades (all $P \leq 0.03$; mean effect on adjusted reaction time = 11.3 ms, $P = 0.06$), but had no effect on search (mean = 0.12%, $P = 0.94$). Thus, our control experiments confirm that the search effect was specific to lesions of the ventral portion of the lateral bank in the IPS (**Fig. 6e**).

In addition, we examined whether our lesion effects were specifically related to GABA modulation. A manganese-only injection (3.0 µl) was made into both LIPd and LIPv (**Supplementary Fig. 3**). There was a slight, nonsignificant improvement on saccade reaction time (−2.2 ms, $P = 0.63$) and error rate (−1.7%, $P = 0.9$; **Supplementary Fig. 3**). Search performance was also unaffected (3.0 ms, $P = 0.46$; −0.4%, $P = 1.0$; **Supplementary Fig. 3**). In contrast, a 1.0-µl muscimol injection into LIPv without manganese impaired both saccades (30.2 ms, $P = 4 \times 10^{-6}$; 8.9%, $P = 0.053$) and search (−4.8 ms, $P = 0.15$; 16.7%, $P = 8 \times 10^{-8}$). A 3.0-µl injection of muscimol alone in LIPd impaired saccades (1.7 ms, $P = 0.4$; 12.9%, $P = 0.0001$), but not search (−1.8 ms, $P = 0.25$; −3.0%, $P = 0.44$). These findings suggest that the lesion effects observed in our experiments specifically resulted from the modulation of GABAergic inhibitory circuits in LIPd or LIPv and that injecting manganese alone into the parietal cortical tissue had minimal effects on saccade and search performance.

DISCUSSION

Our results indicate that well-localized injections of the $GABA_A$ agonist muscimol into LIPd specifically impair saccades, but leave search intact. In contrast, well-localized injections into LIPv impair both search and saccades. There have been two previous reversible inactivation studies of LIP. Both our finding of saccade deficits in LIPd and LIPv and our finding of search deficits in LIPv are consistent with these studies[13–15], although these studies did not distinguish between LIPd and LIPv and did not test for an anatomical gradient of their lesion effects. A previous study[15] reported no significant effect of LIP lesions on saccade reaction time at the population level, but did not report data from individual injections.

The visual search procedure that we employed is the previously described[13] 'difficult feature search', in which search time depends on the number of distractors. We confirmed that this was the case in our monkeys before collecting lesion data and then compared search performance after each lesion in the presence and absence of distractors. This controls for the effects of saccades *per se* and isolates a cost that is ascribed to the role of attention. Because visual search involves many different processes, our results and those of previous studies could conceivably reflect an impairment of, for example, shape processing[29]. However, the most likely explanation for the search effect that we found in LIPv is an impairment of attentional control (see also **Supplementary Text**).

Our muscimol and manganese-enhanced MRI technique allowed us to distinguish the different functional roles of dorsal and ventral LIP. This technique substantially improves the traditional reversible inactivation technique that is used for closely spaced areas and regions in which areal boundaries are not obvious and can resolve controversial issues regarding the functions of other regions such as dorsolateral prefrontal cortex.

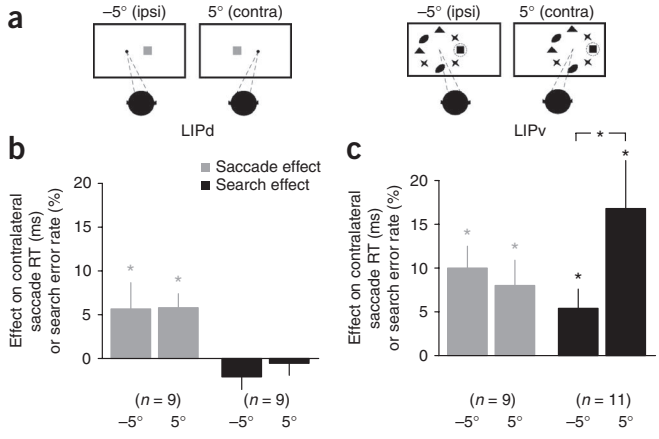

Figure 4 Initial eye position modulates search, but not saccade, effect. (**a**) Initial eye position and all visual stimuli were displaced either 5° to the left or right for both memory-guided saccade task and visual search task. (**b**,**c**) The mean effect with different eye positions on saccade reaction time (gray) and search error rate (black) in LIPd and LIPv. Error bars are 1 s.e.m. *$P < 0.05$.

Areal distinctions

LIPd and LIPv have not been well studied as separate areas. Although they have much in common, they have differences in connectivity and physiology. Anatomically, LIPv is more strongly connected with V3, PIP and PO, whereas LIPd is more strongly connected with V4, V4t, TEa/m, TPOr and area 45 (ref. 21). Both areas are connected to frontal areas close to the FEF[9,21,23], with LIPv being more strongly connected with the caudal periarcuate area[23] and ventral frontal eye fields (areas 45 and 6Vam)[21]. Although LIPd is more strongly connected with the rostral periarcuate area (intermediate area 8)[23] and dorsal frontal eye field (8Ac, 8As)[21], overall stronger connections from LIPv to FEF have been reported[30]. FEF has been traditionally viewed as an oculomotor structure, but it has been recently implicated in attentional processing[31–33]. This dual role is consistent with our finding of both saccade and search effects after LIPv lesions. LIP also has direct projections to the superior colliculus[7]. Similar to FEF, superior colliculus has been traditionally viewed as an oculomotor structure and has also been recently implicated in attentional processing[34,35]. The LIP neurons projecting to FEF and superior colliculus are intermingled[36], but there appears to be a stronger projection to the intermediate and deep layers of the superior colliculus from deeper areas in the lateral bank, approximately corresponding to LIPv[7].

In summary, LIPv, when compared with LIPd, has stronger connections to FEF and superior colliculus and weaker connections

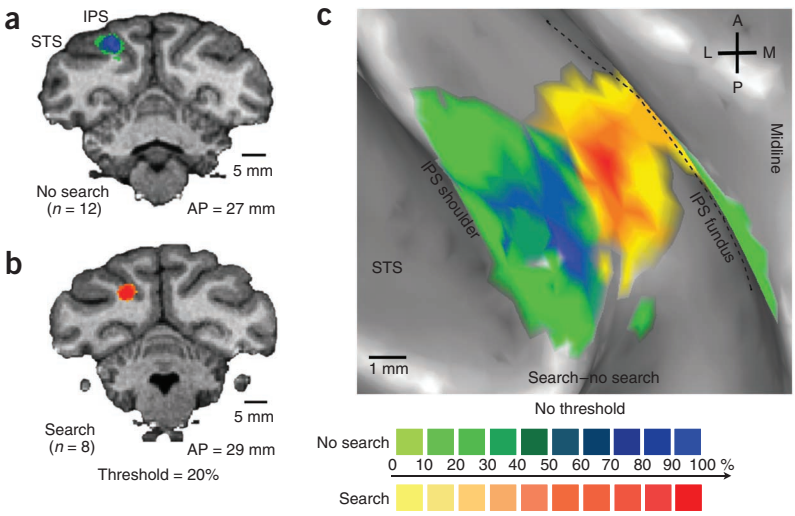

Figure 5 Lesion overlap maps. (**a**,**b**) The estimated areas of inactivation (see **Supplementary Text**) for all search-negative (**a**) and search-positive (**b**) injections from two fascicularis monkeys are shown on coronal brain slices. The color palette indicates the percentage of search-negative or search-positive lesions that involved each voxel. Data are thresholded at 20%. (**c**) The voxel-wise percentage effects from **a** and **b** were subtracted and projected, without thresholding, onto the inflated cortical surface. A, anterior; L, lateral; M, medial; P, posterior; STS, superior temporal sulcus.

to V4. This is surprising given our results and the classic view of FEF and superior colliculus as being oculomotor related and V4 as being attention related. This surprise is mitigated, however, by the fact that superior colliculus, FEF and V4 all show both oculomotor and attentional effects[34,35,37] and that FEF is itself strongly connected with V4 (refs. 10,30). Furthermore, it has been previously suggested that LIPv is involved in complex cognitive functions, such as integrating sensory evidence and engaging and disengaging attention[38–40]. Functionally, single-unit recording studies have suggested that LIPv represents the periphery, whereas LIPd represents the fovea[9,41], but we did not find evidence for impaired foveal stability after either LIPd or LIPv lesions (see **Supplementary Text** and **Supplementary Fig. 4**).

Functional specificity at the area and circuit levels

There has been a long-standing debate about whether LIP has a specific oculomotor role[1,2,5,12,14] or is involved in allocating attention, perhaps by providing a general salience map of visual space[3,4,6,13,15]. A number of studies have attempted to separate saccadic from attentional processing[4,20]. The locus of attention can be continuously tracked using psychophysical techniques, but saccadic intention is much more difficult to measure. Activity in LIP tracks the time course of attention[4], predicts the goal and latency of upcoming saccades under conditions of free visual search[42] but not when a task-irrelevant stimulus appears near the end of the delay period of a memory-guided delayed saccade[43], and distinguishes between targets and distractors during visual search[44]. Our findings suggest that LIP is involved in both attention and saccade intention. Our lesion data confirm this, consistent with previous studies that found an intimate relationship between the saccade and attention systems at the level of both behavior[17] and neural circuitry[18,19].

The effects that we observed of LIP lesions on saccades and search were very small but reliable (for example, 5–10 ms increases in latency). The search effects that we observed and that have been reported previously[13] were comparable to those of FEF inactivations[45], but the saccade effects were at least an order of magnitude smaller than those of FEF[45,46] and superior colliculus inactivations[47], and lesions in these areas also impaired saccade metrics. This is consistent with the notion that LIP helps specify saccadic goals but, unlike FEF and superior colliculus, is not directly involved in generating the saccade itself. In addition, parallel pathways that bypass LIP may exist for specifying saccade goals, which could compensate for the loss of function after LIP lesions. Finally, superior colliculus and, to a lesser extent, FEF are more highly topographically organized than LIP, and circumscribed lesions may have pronounced focal effects in superior colliculus and FEF and more diffuse effects in LIP.

Our data suggest that there may be separate neural substrates for oculomotor and attentional functions in LIPv, similar to what has been found in FEF[31,32]. LIPd and LIPv lesions affected saccade reaction time more reliably than the saccade error rate, whereas LIPv lesions affected search error rate more strongly than reaction time. Notably, eye position modulated the search effect but not the saccade effect (**Fig. 4c**). The lack of an eye position effect on saccades is consistent with previous results[48], whereas the eye position effect on visual search is consistent with the fact that hemineglect in humans is often modulated by eye position[49,50]. We propose that there are two intermingled cell populations in LIPv, similar to what has been found in FEF[31], with one group of cells being involved in saccade planning and the other being involved in spatial attention.

In summary, we found different functional roles for the two subdivisions of LIP. LIPd is primarily an oculomotor planning region and LIPv is involved in both oculomotor and attentional processing. Thus, oculomotor processing can exist independently of attentional processing in the posterior parietal cortex (LIPd), but the two processes can also operate side-by-side in the same cortical area (LIPv). Furthermore, when both processes are present in the same area, they

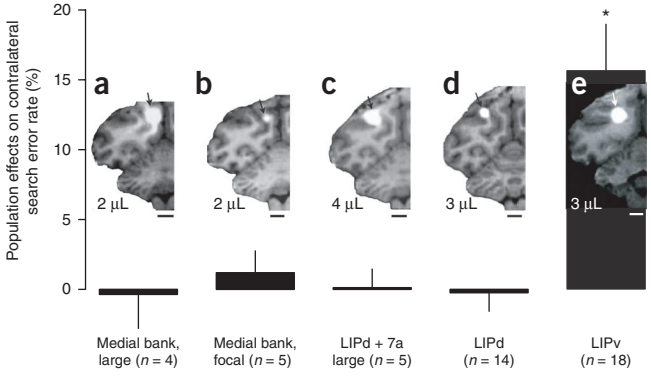

Figure 6 MRIs and search effects of control injections. (**a**–**e**) Control injections were grouped into large medial bank (**a**), focal medial bank (**b**), large LIPd + 7a (**c**), LIPd (**d**) and LIPv (**e**) injections. Bars and error bars show the population effects of each injection type on search error rates in the contralateral hemifield. Error bars are one s.e.m. Scale bars represent 5 mm. Only LIPv injections produced a significant increase in search error rate (*$P < 0.0001$). Data from the five large LIPd + 7a injections are included in the LIPd data.

appear to be subserved by independent neural elements (LIPv and FEF). This architecture may provide a flexible neuronal substrate for switching between coupling and decoupling of covert attention and eye movements[18,19,31].

METHODS

Methods and any associated references are available in the online version of the paper at http://www.nature.com/natureneuroscience/.

Note: Supplementary information is available on the Nature Neuroscience website.

ACKNOWLEDGMENTS

We thank J. Baker and G. Patel for assistance in developing the manganese-MRI technique, and T. Malone, J. Tucker and J. Vytlacil for technical assistance. This work was supported by National Eye Institute grant EY012135 and National Science Foundation (Integrative Graduate Education and Research Traineeship) grant 0548890.

AUTHOR CONTRIBUTIONS

Y.L. performed all aspects of this study, including the experimental design, data collection of two monkeys, analysis and writing of the manuscript. E.A.Y. assisted in data collection and analysis. L.H.S. oversaw the experiments and assisted in data analysis and manuscript preparation.

COMPETING FINANCIAL INTERESTS

The authors declare no competing financial interests.

Published online at http://www.nature.com/natureneuroscience/.
Reprints and permissions information is available online at http://www.nature.com/reprintsandpermissions/.

1. Barash, S., Bracewell, R.M., Fogassi, L., Gnadt, J.W. & Andersen, R.A. Saccade-related activity in the lateral intraparietal area. II. Spatial properties. *J. Neurophysiol.* **66**, 1109–1124 (1991).
2. Snyder, L.H., Batista, A.P. & Andersen, R.A. Coding of intention in the posterior parietal cortex. *Nature* **386**, 167–170 (1997).
3. Gottlieb, J.P., Kusunoki, M. & Goldberg, M.E. The representation of visual salience in monkey parietal cortex. *Nature* **391**, 481–484 (1998).
4. Bisley, J.W. & Goldberg, M.E. Neuronal activity in the lateral intraparietal area and spatial attention. *Science* **299**, 81–86 (2003).
5. Thier, P. & Andersen, R.A. Electrical microstimulation distinguishes distinct saccade-related areas in the posterior parietal cortex. *J. Neurophysiol.* **80**, 1713–1735 (1998).
6. Cutrell, E.B. & Marrocco, R.T. Electrical microstimulation of primate posterior parietal cortex initiates orienting and alerting components of covert attention. *Exp. Brain Res.* **144**, 103–113 (2002).
7. Lynch, J.C., Graybiel, A.M. & Lobeck, L.J. The differential projection of two cytoarchitectonic subregions of the inferior parietal lobule of macaque upon the deep layers of the superior colliculus. *J. Comp. Neurol.* **235**, 241–254 (1985).
8. Tanné, J., Boussaoud, D., Boyer-Zeller, N. & Rouiller, E.M. Direct visual pathways for reaching movements in the macaque monkey. *Neuroreport* **7**, 267–272 (1995).
9. Blatt, G.J., Andersen, R.A. & Stoner, G.R. Visual receptive field organization and cortico-cortical connections of the lateral intraparietal area (area LIP) in the macaque. *J. Comp. Neurol.* **299**, 421–445 (1990).
10. Stanton, G.B., Bruce, C.J. & Goldberg, M.E. Topography of projections to posterior cortical areas from the macaque frontal eye fields. *J. Comp. Neurol.* **353**, 291–305 (1995).
11. Rushworth, M.F., Nixon, P.D. & Passingham, R.E. Parietal cortex and movement. I. Movement selection and reaching. *Exp. Brain Res.* **117**, 292–310 (1997).
12. Chafee, M.V. & Goldman-Rakic, P.S. Inactivation of parietal and prefrontal cortex reveals interdependence of neural activity during memory-guided saccades. *J. Neurophysiol.* **83**, 1550–1566 (2000).
13. Wardak, C., Olivier, E. & Duhamel, J.R. A deficit in covert attention after parietal cortex inactivation in the monkey. *Neuron* **42**, 501–508 (2004).
14. Li, C.S., Mazzoni, P. & Andersen, R.A. Effect of reversible inactivation of macaque lateral intraparietal area on visual and memory saccades. *J. Neurophysiol.* **81**, 1827–1838 (1999).
15. Wardak, C., Olivier, E. & Duhamel, J.R. Saccadic target selection deficits after lateral intraparietal area inactivation in monkeys. *J. Neurosci.* **22**, 9877–9884 (2002).
16. Posner, M.I. Orienting of attention. *Q. J. Exp. Psychol.* **32**, 3–25 (1980).
17. Land, M.F. & Hayhoe, M. In what ways do eye movements contribute to everyday activities? *Vision Res.* **41**, 3559–3565 (2001).
18. Kustov, A.A. & Robinson, D.L. Shared neural control of attentional shifts and eye movements. *Nature* **384**, 74–77 (1996).
19. Corbetta, M. *et al.* A common network of functional areas for attention and eye movements. *Neuron* **21**, 761–773 (1998).
20. Kowler, E., Anderson, E., Dosher, B. & Blaser, E. The role of attention in the programming of saccades. *Vision Res.* **35**, 1897–1916 (1995).
21. Lewis, J.W. & Van Essen, D.C. Corticocortical connections of visual, sensorimotor and multimodal processing areas in the parietal lobe of the macaque monkey. *J. Comp. Neurol.* **428**, 112–137 (2000).
22. Lewis, J.W. & Van Essen, D.C. Mapping of architectonic subdivisions in the macaque monkey, with emphasis on parieto-occipital cortex. *J. Comp. Neurol.* **428**, 79–111 (2000).
23. Medalla, M. & Barbas, H. Diversity of laminar connections linking periarcuate and lateral intraparietal areas depends on cortical structure. *Eur. J. Neurosci.* **23**, 161–179 (2006).
24. Cox, D.D., Papanastassiou, A.M., Oreper, D., Andken, B.B. & Dicarlo, J.J. High-resolution three-dimensional microelectrode brain mapping using stereo microfocal X-ray imaging. *J. Neurophysiol.* **100**, 2966–2976 (2008).
25. Koretsky, A.P. & Silva, A.C. Manganese-enhanced magnetic resonance imaging (MEMRI). *NMR Biomed.* **17**, 527–531 (2004).
26. Desimone, R. & Duncan, J. Neural mechanisms of selective visual attention. *Annu. Rev. Neurosci.* **18**, 193–222 (1995).
27. Schneider, W. & Schiffrin, R.M. Controlled and automatic human information processing: I. Detection, search and attention. *Psychol. Rev.* **84**, 1–66 (1977).
28. Andersen, R.A., Bracewell, R.M., Barash, S., Gnadt, J.W. & Fogassi, L. Eye position effects on visual, memory and saccade-related activity in areas LIP and 7a of macaque. *J. Neurosci.* **10**, 1176–1196 (1990).
29. Sereno, A.B. & Maunsell, J.H. Shape selectivity in primate lateral intraparietal cortex. *Nature* **395**, 500–503 (1998).
30. Schall, J.D., Morel, A., King, D.J. & Bullier, J. Topography of visual cortex connections with frontal eye field in macaque: convergence and segregation of processing streams. *J. Neurosci.* **15**, 4464–4487 (1995).
31. Murthy, A., Thompson, K.G. & Schall, J.D. Dynamic dissociation of visual selection from saccade programming in frontal eye field. *J. Neurophysiol.* **86**, 2634–2637 (2001).
32. Moore, T., Armstrong, K.M. & Fallah, M. Visuomotor origins of covert spatial attention. *Neuron* **40**, 671–683 (2003).
33. Moore, T. & Fallah, M. Microstimulation of the frontal eye field and its effects on covert spatial attention. *J. Neurophysiol.* **91**, 152–162 (2004).
34. Müller, J.R., Philiastides, M.G. & Newsome, W.T. Microstimulation of the superior colliculus focuses attention without moving the eyes. *Proc. Natl. Acad. Sci. USA* **102**, 524–529 (2005).
35. Ignashchenkova, A., Dicke, P.W., Haarmeier, T. & Thier, P. Neuron-specific contribution of the superior colliculus to overt and covert shifts of attention. *Nat. Neurosci.* **7**, 56–64 (2004).
36. Gaymard, B., Lynch, J., Ploner, C.J., Condy, C. & Rivaud-Pechoux, S. The parieto-collicular pathway: anatomical location and contribution to saccade generation. *Eur. J. Neurosci.* **17**, 1518–1526 (2003).
37. Moore, T. & Armstrong, K.M. Selective gating of visual signals by microstimulation of frontal cortex. *Nature* **421**, 370–373 (2003).
38. Yang, T. & Shadlen, M.N. Probabilistic reasoning by neurons. *Nature* **447**, 1075–1080 (2007).
39. Huk, A.C. & Shadlen, M.N. Neural activity in macaque parietal cortex reflects temporal integration of visual motion signals during perceptual decision making. *J. Neurosci.* **25**, 10420–10436 (2005).
40. Ben Hamed, S. & Duhamel, J.R. Ocular fixation and visual activity in the monkey lateral intraparietal area. *Exp. Brain Res.* **142**, 512–528 (2002).
41. Ben Hamed, S., Duhamel, J.R., Bremmer, F. & Graf, W. Representation of the visual field in the lateral intraparietal area of macaque monkeys: a quantitative receptive field analysis. *Exp. Brain Res.* **140**, 127–144 (2001).
42. Ipata, A.E., Gee, A.L., Goldberg, M.E. & Bisley, J.W. Activity in the lateral intraparietal area predicts the goal and latency of saccades in a free-viewing visual search task. *J. Neurosci.* **26**, 3656–3661 (2006).
43. Powell, K.D. & Goldberg, M.E. Response of neurons in the lateral intraparietal area to a distractor flashed during the delay period of a memory-guided saccade. *J. Neurophysiol.* **84**, 301–310 (2000).
44. Ipata, A.E., Gee, A.L., Bisley, J.W. & Goldberg, M.E. Neurons in the lateral intraparietal area create a priority map by the combination of disparate signals. *Exp. Brain Res.* **192**, 479–488 (2009).
45. Wardak, C., Ibos, G., Duhamel, J.R. & Olivier, E. Contribution of the monkey frontal eye field to covert visual attention. *J. Neurosci.* **26**, 4228–4235 (2006).
46. Dias, E.C. & Segraves, M.A. Muscimol-induced inactivation of monkey frontal eye field: effects on visually and memory-guided saccades. *J. Neurophysiol.* **81**, 2191–2214 (1999).
47. Aizawa, H. & Wurtz, R.H. Reversible inactivation of monkey superior colliculus. I. Curvature of saccadic trajectory. *J. Neurophysiol.* **79**, 2082–2096 (1998).
48. Li, C.S. & Andersen, R.A. Inactivation of macaque lateral intraparietal area delays initiation of the second saccade predominantly from contralesional eye positions in a double-saccade task. *Exp. Brain Res.* **137**, 45–57 (2001).
49. Vuilleumier, P. & Schwartz, S. Modulation of visual perception by eye gaze direction in patients with spatial neglect and extinction. *Neuroreport* **12**, 2101–2104 (2001).
50. Pavani, F., Ladavas, E. & Driver, J. Gaze direction modulates auditory spatial deficits in stroke patients with neglect. *Cortex* **41**, 181–188 (2005).

ONLINE METHODS

Three adult male macaque monkeys (two *Macaca fascicularis*, monkeys Q and W; one *Macaca mulatta*, monkey G) were used. All procedures conformed to the *Guide for the Care and Use of Laboratory Animals* and were approved by the Washington University Institutional Animal Care and Use Committee.

Delineation of LIP. We localized LIP in four hemispheres of three monkeys using MRI and single-neuron recording. LIP was defined as a zone in the lateral bank of the IPS, close to the bend in the sulcus, that contained a high proportion of cells with a brisk phasic response to onset of a visual target in the receptive field and significantly elevated ($P < 0.05$) activity during the delay period of a memory-guided saccade task (**Supplementary Fig. 5**).

Injections. We injected 8 mg ml^{-1} muscimol and 0.1 M manganese (19.8 mg ml^{-1} $MnCl_2(H_2O)_4$) in sterile water at 0.1 µl min^{-1} using a microinjection pump (Harvard Apparatus HA11D). A total of 8–32 µg of muscimol (median, 16 µg) was injected per experiment. Injections were made through a chamber mounted over LIP using a custom assembly consisting of 33-gauge hypodermic tubing connected to a 25-µl Hamilton syringe. Injection coordinates were selected on the basis of pre-injection mapping experiments (see **Supplementary Fig. 5**) and on animal-specific MRI atlases. For each experiment, 1 or 2 µl of muscimol and manganese were injected at one to four sites along one or two injection tracks, for a total volume of 1–4 µl per experiment.

The volumes of injections placed in the two areas were comparable (mean ± s.d., 2.6 ± 0.9 (mode, 2) µl for LIPd and 2.2 ± 0.9 (mode, 2) µl for LIPv). The cannula was withdrawn 15 min after the completion of each injection. Injections were visible as bright halos representing the manganese-induced T1 signal increase.

Part of our motivation in developing the muscimol and manganese MRI technique was to be able to detect any leakage of the drug along the injection track into regions distant from the intended injection site. Such leakage, which cannot be detected with traditional injection methods, limits the interpretation of all previous inactivation studies. In contrast with the manganese MRI technique, any substantial leakage that occurs during cannula advancement and/or injection or any backfilling that occurs during cannula retraction is clearly visible in the post-injection MRI. An example of this is shown in **Supplementary Figure 6**. Injections that showed any sign of leakage along the cannula track or that failed to show a visible halo were excluded from our dataset.

Only a single site (LIPd or LIPv) was tested in each injection session. Typically, one injection and two control sessions were performed each week. The order of injections into LIPd and LIPv was intentionally varied for each monkey to avoid systematic biases (d, LIPd; v, LIPv; Monkey Q: v, v, v, d, d, d, d, v, d, v, v, d, d, v and v; Monkey W: v, v, v, d and d; Monkey G: d, d, d, d, d, v, v, d, d, v, v, v, v, v and d). We found only small and nonsystematic changes in the injection effects as a function of session number (see **Supplementary Text** and **Supplementary Fig. 7**).

Behavioral tasks. Two male *Macaca fascicularis* and one male *Macaca mulatta* monkey performed a standard memory-guided saccade task[2] and a visual-search task (adapted from refs. 13,15) in control and injection sessions. Memory trials began with the monkey looking at a fixation point on a vertically mounted screen 16 cm away. After 350-ms fixation, a peripheral target appeared for 150 ms in one of eight directions 20° from the fixation point. After a subsequent 1–1.6-s delay, the fixation light was extinguished and the monkey had 500 ms to saccade to within 10° of the remembered target location. The target reappeared 150 ms after the eyes acquired the peripheral window and a corrective saccade to within 5° was required. Early (before fixation offset), late (>500 ms), inaccurate (>10° from target) or failed corrective saccades were counted as errors. A total of 240 correct saccades were obtained per experimental session. Memory reach trials were interleaved with the memory saccade trials.

In the visual-search task, after 800–1,300 ms of central fixation, the fixation point was extinguished and a search array appeared. On two-thirds of trials, a purple square and seven equally spaced purple distractors with three different shapes appeared at 12° or 15° eccentricity. On one-third of trials, the target appeared without distractors. Monkeys were rewarded for directing a single saccade to within 6° of the target. Trials were terminated if the monkey saccaded to a distractor or made more than one saccade. A total of 144 trials without distrators and 288 trials with distractors were obtained in each experimental session.

To test whether initial eye position would modulate lesion effects, two monkeys performed separate blocks of the saccade and search tasks using starting eye positions and visual stimuli 5° to the right or left of straight ahead.

Because the effects of the muscimol might change over time, the first two monkeys (Q and W) performed multiple blocks of tasks, with each block (45 min) consisting of three tasks running sequentially. The three tasks were interleaved: visual saccades and reaches, interleaved memory saccades and reaches, and visual search. Initial eye position (5° to the right or left of straight ahead) was alternated on each consecutive set. A total of six blocks of data were collected in each control and injection experiment, lasting 4–5 h. The third monkey (G) performed only a single block of interleaved memory saccades and reaches and a single block of visual search in each session. The first three injections were performed in monkey G before it was fully trained on the search task, and therefore only saccade data were collected in those three experiments.

Behavioral data analysis. Injection session data were compared with data from two to four control sessions from adjacent days within 2 weeks of the injection day, so that cumulative lesion effects would not bias our results (see also **Supplementary Text** and **Supplementary Fig. 7**). Errors that occurred before target appearance on memory and search trials were excluded from error analysis. Saccade errors include fixation errors (errors caused by eye movements, occurring at any time between the transient peripheral target presentation and the fixation point offset), target acquisition errors (failure to move the eyes to within 10° of the remembered peripheral target location in 500 ms of fixation point offset) and late errors (failure to maintain fixation on the peripheral target for at least 150 ms or a failure to make a corrective saccade to within 5° of the visible peripheral target location after it reappeared at the end of the trial). Search errors occurred when a saccade was landed more than 6° from the target, or when the first saccade was landed on a distractor. The saccade onset was defined as the time at which eye velocity first exceeded 30° s^{-1}, and saccade offset was defined as the time when eye velocity dropped below 24° s^{-1}. Movement amplitude was defined as the Euclidean distance from starting point to ending point. Precision was assessed by the variability of movement amplitude. To exclude oculomotor effects from the search task reaction time and error measurements, we subtracted no-distractor data from seven-distractor data, leaving only the influence of the distractors (adapted from ref. 15). For comparisons of reaction time (fixation offset to saccade onset, reaction time), amplitude and duration, we parceled out between control days and within control day variances, then used the control mean, the within control day variance, the injection mean and the injection variance to compute two-sided Welch's *t*-test *P* values. For the comparison of the variability of movement amplitude (precision), we used the within control day variance and the injection day variance to compute two-sided *F* (variance ratio) test. We used two-sided χ^2 tests (or Fisher exact tests if any of the expected counts were less than 5) for individual site error rate comparisons. Significant sites were the ones that significantly delayed reaction time or increased errors ($P < 0.05$, corrected for multiple comparisons of two). Population effects across injections were tested using a one sample two-sided permutation test. Single-sided tests would be appropriate for all of these comparisons, so the *P* values from the two-sided tests are generally conservative. Unless otherwise mentioned, statistics were computed for the three contralateral target positions.

Image acquisition and analysis. Post-injection (4–8 h) magnetic resonance scans (T1 weighted, magnetization prepared rapid acquisition gradient echo pulse sequences) were performed with a Siemens Allegra 3T MRI scanner (Siemens Medical Systems) using a custom volumetric 'birdcage' coil (14-cm inner diameter, Primatrix). For about two thirds of the scans (25 of 35), monkeys were sedated (10–15 mg per kg of body weight ketamine and 0.7–1.0 mg per kg diazepam) or anesthetized with isoflurane and monitored using an magnetic resonance–compatible pulse-oximetry probe (Surgivet). Ten scans were acquired while the monkeys were fully awake. Typically, three 8-min scans at 0.5-mm^3 resolution were acquired with anesthesia and six 3-min scans at 1.0-mm^3 resolution were acquired without anesthesia. See **Supplementary Text** for image processing.

Injection depth was measured as the Euclidean distance from the center of each manganese halo to the adjacent gyral surface of the intraparietal sulcus, normalized by dividing by the full IPS sulcal depth (**Fig. 2**) and multiplying by the mean full depth across the three monkeys (8.9, 17.6 and 12.0 mm, for a mean of 12.8 mm). All depths in the text have been normalized in this

manner. Normalization had only a very small effect on the results and the distinction between LIPd and LIPv injections was just as clear using non-normalized values. All depth measurements were made in the coronal plane. To locate the depth of the LIPd/v boundary in previous anatomical data[21,22], we first converted the two-dimensional fascicularis cytoarchitectonic parcellation into a three-dimensional volume (CARET, http://brainvis.wustl.edu, sum database: Macaque.F6.BOTH.Std-MESH.73730) and then computed the normalized depth of the border. We estimated the LIPd/v boundary as lying about 4.6 mm deep in the MRI atlas (full IPS depth, 8.7 mm) and 6.8 mm deep for the normalized sulcal depth of our monkeys (12.8 mm). All LIP injections were located near the middle of the IPS where the sulcus is relatively straight (for example, **Fig. 2**), so sulcal curvature was not an issue in our measurements.

The normalized anterior-to-posterior distance for each injection was computed as the distance of the center of the manganese halo to the junction of IPS and parietal occipital sulcus, relative to that animal's full anterior-to-posterior IPS length (**Supplementary Text** and **Supplementary Figs. 8** and **9**). These measurements were made in the horizontal plane.

doi:10.1038/nn.2496